# $GABA_B$ receptor deficiency causes failure of neuronal homeostasis in hippocampal networks

Irena Vertkin[a], Boaz Styr[a], Edden Slomowitz[a], Nir Ofir[a,b], Ilana Shapira[a], David Berner[c], Tatiana Fedorova[a,b], Tal Laviv[a,b,1], Noa Barak-Broner[a], Dafna Greitzer-Antes[a,2], Martin Gassmann[c], Bernhard Bettler[c], Ilana Lotan[a,b], and Inna Slutsky[a,b,3]

[a]Department of Physiology and Pharmacology, Sackler Faculty of Medicine, Tel Aviv University, 69978 Tel Aviv, Israel; [b]Sagol School of Neuroscience, Tel Aviv University, 69978 Tel Aviv, Israel; and [c]Department of Biomedicine, Institute of Physiology, Pharmazentrum, University of Basel, CH-4056 Basel, Switzerland

Edited by Gina G. Turrigiano, Brandeis University, Waltham, MA, and approved May 14, 2015 (received for review January 8, 2015)

**Stabilization of neuronal activity by homeostatic control systems is fundamental for proper functioning of neural circuits. Failure in neuronal homeostasis has been hypothesized to underlie common pathophysiological mechanisms in a variety of brain disorders. However, the key molecules regulating homeostasis in central mammalian neural circuits remain obscure. Here, we show that selective inactivation of $GABA_B$, but not $GABA_A$, receptors impairs firing rate homeostasis by disrupting synaptic homeostatic plasticity in hippocampal networks. Pharmacological $GABA_B$ receptor ($GABA_BR$) blockade or genetic deletion of the $GB_{1a}$ receptor subunit disrupts homeostatic regulation of synaptic vesicle release. $GABA_BRs$ mediate adaptive presynaptic enhancement to neuronal inactivity by two principle mechanisms: First, neuronal silencing promotes syntaxin-1 switch from a closed to an open conformation to accelerate soluble N-ethylmaleimide-sensitive factor attachment protein receptor (SNARE) complex assembly, and second, it boosts spike-evoked presynaptic calcium flux. In both cases, neuronal inactivity removes tonic block imposed by the presynaptic, $GB_{1a}$-containing receptors on syntaxin-1 opening and calcium entry to enhance probability of vesicle fusion. We identified the $GB_{1a}$ intracellular domain essential for the presynaptic homeostatic response by tuning intermolecular interactions among the receptor, syntaxin-1, and the $Ca_V2.2$ channel. The presynaptic adaptations were accompanied by scaling of excitatory quantal amplitude via the postsynaptic, $GB_{1b}$-containing receptors. Thus, $GABA_BRs$ sense chronic perturbations in GABA levels and transduce it to homeostatic changes in synaptic strength. Our results reveal a novel role for $GABA_BR$ as a key regulator of population firing stability and propose that disruption of homeostatic synaptic plasticity may underlie seizure's persistence in the absence of functional $GABA_BRs$.**

homeostatic plasticity | $GABA_B$ receptor | synaptic vesicle release | syntaxin-1 | FRET

Neural circuits achieve an ongoing balance between plasticity and stability to enable adaptations to constantly changing environments while maintaining neuronal activity within a stable regime. Hebbian-like plasticity, reflected by persistent changes in synaptic and intrinsic properties, is crucial for refinement of neural circuits and information storage; however, alone it is unlikely to account for the stable functioning of neural networks (1). In the last 2 decades, major progress has been made toward understanding the homeostatic negative feedback systems underlying restoration of a baseline neuronal function after prolonged activity perturbations (2–4). Homeostatic processes may counteract the instability by adjusting intrinsic neuronal excitability, inhibition-to-excitation balance, and synaptic strength via postsynaptic or presynaptic modifications (5, 6) through a profound molecular reorganization of synaptic proteins (7, 8). These stabilizing mechanisms have been collectively termed homeostatic plasticity. Homeostatic mechanisms enable invariant firing rates and patterns of neural networks composed from intrinsically unstable activity patterns of individual neurons (9).

However, nervous systems are not always capable of maintaining constant output. Although some mutations, genetic knockouts, or pharmacologic perturbations induce a compensatory response that restores network firing properties around a predefined "set point" (10), the others remain uncompensated, or their compensation leads to pathological function (11). The inability of neural networks to compensate for a perturbation may result in epilepsy and various types of psychiatric disorders (12). Therefore, determining under which conditions activity-dependent regulation fails to compensate for a perturbation and identifying the key regulatory molecules of neuronal homeostasis is critical for understanding the function and malfunction of central neural circuits.

In this work, we explored the mechanisms underlying the failure in stabilizing hippocampal network activity by combining long-term extracellular spike recordings by multielectrode arrays (MEAs), intracellular patch-clamp recordings of synaptic responses, imaging of synaptic vesicle exocytosis, and calcium dynamics, together with FRET-based analysis of intermolecular interactions at individual synapses. Our results demonstrate that metabotropic, G protein-coupled receptors for GABA, $GABA_BRs$, are essential for firing rate homeostasis in hippocampal networks. We explored the mechanisms by which $GABA_BRs$ gate homeostatic synaptic

## Significance

How neuronal circuits maintain stable activity despite continuous environmental changes is one of the most intriguing questions in neuroscience. Previous studies proposed that deficits in homeostatic control systems may underlie common neurological symptoms in a variety of brain disorders. However, the key regulatory molecules that control homeostasis of central neural circuits remain obscure. We show here that basal activity of $GABA_B$ receptors is required for firing rate homeostasis in hippocampal networks. We identified the principal mechanisms by which $GABA_B$ receptors control homeostatic augmentation of synaptic strength to chronic neuronal silencing. We propose that deficits in $GABA_B$ receptor signaling, associated with epilepsy and psychiatric disorders, may lead to aberrant brain activity by erasing homeostatic plasticity.

Author contributions: I.V. and I. Slutsky designed research; I.V., B.S., E.S., N.O., I. Shapira, D.B., T.F., and T.L. performed research; N.B.-B., D.G.-A., M.G., B.B., and I.L. contributed new reagents/analytic tools; I.V., B.S., E.S., N.O., I. Shapira, D.B., T.F., T.L., M.G., B.B., and I. Slutsky analyzed data; and I.V. and I. Slutsky wrote the paper.

The authors declare no conflict of interest.

This article is a PNAS Direct Submission.

Freely available online through the PNAS open access option.

[1]Present address: Max Planck Florida Institute for Neuroscience, Jupiter, FL 33468-0998.

[2]Present address: Department of Medicine, University of Toronto, Toronto, ON, Canada M5S 1A8.

[3]To whom correspondence should be addressed. Email: islutsky@post.tau.ac.il.

This article contains supporting information online at www.pnas.org/lookup/suppl/doi:10.1073/pnas.1424810112/-/DCSupplemental.

plasticity. Our study raises the possibility that persistence of epileptic seizures in $GABA_BR$-deficient mice (13–15) is directly linked to impairments in a homeostatic control system.

## Results

**$GABA_BR$ Blockade Disrupts Firing Rate Homeostasis.** Mice lacking functional $GABA_BRs$ because of $GB_1$ or $GB_2$ subunit deletion display continuous spontaneous seizure activity (13–16). These findings are quite counterintuitive in light of a wide range of G protein-coupled receptors that mediate synaptic inhibition and might compensate for $GABA_BR$ loss of function. Therefore, we hypothesized that functional $GABA_BRs$ may play an essential role in neuronal homeostasis. To test this hypothesis, we examined homeostasis of mean firing rate of a neuronal population after chronic blockade of $GABA_BRs$. To chronically monitor neuronal activity in stable neural populations, we grew hippocampal cultures on MEAs for ~3 wk. Each MEA contains 59 recording electrodes, with each electrode capable of recording the activity of several adjacent neurons (Fig. 1*A*). Spikes were detected and analyzed using principal component analysis to obtain well-separated single units that were consistent throughout at least 2 d of recording (*SI Appendix*, *Methods*). To assess how chronic inhibition of the basal $GABA_BR$ activity affects mean firing rate of neural network, we measured spiking activity during a baseline recording period and for 2 d after application of CGP54626 (CGP), a selective $GABA_BR$ antagonist. Fig. 1*B* illustrates raster plots during periods of baseline, 1 h, and 48 h after 1 μM CGP application in a single experiment. Indeed, CGP causes an acute increase of 67 ± 13% in the mean firing rate (Fig. 1*C*), confirming proconvulsive properties of $GABA_BR$ antagonists in vivo (17). However, to our surprise, mean firing rate was not normalized during 2 d in the constant presence of CGP. After 2 d, firing rate remained 67 ± 18% higher in the presence of $GABA_BR$ antagonist ($P < 0.01$; Fig. 1*C*). Notably, under control conditions, network spike rates were stable during the 2 d of recording (no treatment, $P > 0.2$ between 1 h and 48 h; Fig. 1*D*).

To confirm that the lack of firing rate homeostasis is specific to the $GABA_BR$ blockade, we examined how chronic blockade of $GABA_ARs$ affects the population firing rate in hippocampal networks. Application of $GABA_AR$ antagonist gabazine (30 μM) caused a fast and pronounced increase in the population firing rate to 330 ± 32%, which gradually declined over the course of 2 d in the presence of gabazine (Fig. 1*E*), despite the constant presence of the antagonist. Washout of gabazine after 2 d caused a significant decrease in firing rate, indicating sustained activity of both gabazine and the $GABA_ARs$ (*SI Appendix*, Fig. S1).

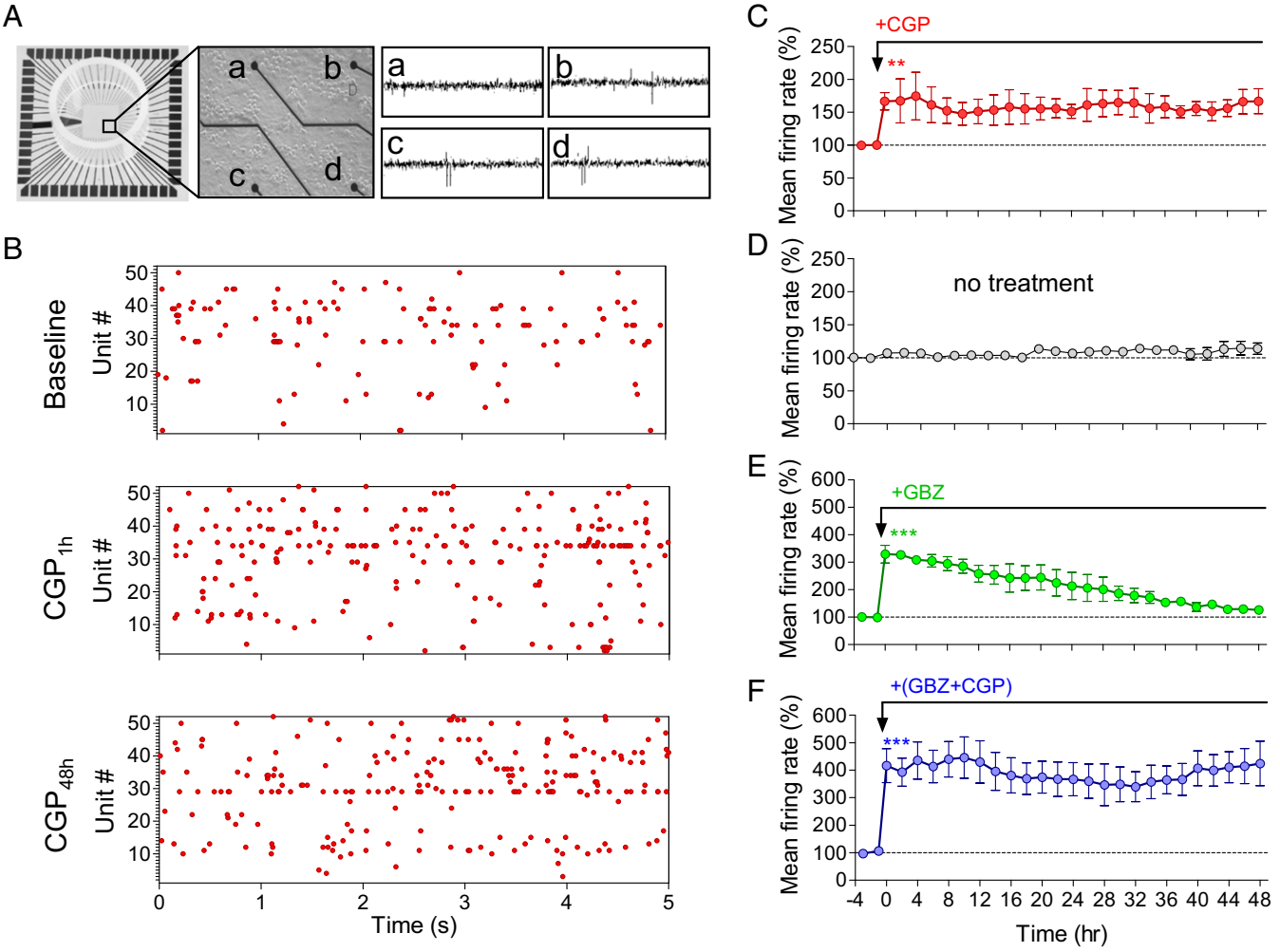


**Fig. 1.** $GABA_BR$ blockade disrupts firing rate homeostasis in hippocampal networks. (*A*, *Left*) Image of MEA dish. (*Middle*) Image of dissociated hippocampal culture plated on MEA. Black circles at the end of the black lines are the recording electrodes. (*Right*) Representative traces of recording from four MEA channels (*a*, *b*, *c*, and *d*). (*B*) Representative raster plot of MEA recording before and 1 and 48 h after application of the $GABA_BR$ antagonist CGP (1 μM). (*C–F*) Mean firing rate of hippocampal neuronal cultures incubated with CGP ($n = 4$; *C*), no treatment (Cnt, $n = 6$; *D*), gabazine (GBZ, 30 μM, $n = 4$; *E*), and CGP+GBZ ($n = 4$; *F*) during 2 d of MEA recordings.

Moreover, a $GABA_BR$ agonist, baclofen, triggered a pronounced block of firing rate that was precisely restored to the baseline level after a period of 2 d (9). The observed compensatory responses to increase in spiking activity by $GABA_AR$ antagonist or decrease in spiking activity by $GABA_BR$ agonist confirm the idea that homeostatic mechanisms maintain stable circuit function by keeping neuronal firing rate around a "set point" (10, 18).

Given a 3.4-fold difference in the magnitude of the initial firing rate increase produced by $GABA_AR$ versus $GABA_BR$ blockade, it is plausible that the lack of firing rate renormalization in the presence of CGP was a result of its relatively weak effect on firing rate. If this is the case, concurrent blockade of $GABA_ARs$ and $GABA_BRs$ would result in a reversal of firing rate, as in the presence of the $GABA_AR$ blocker alone. However, coapplication of gabazine and CGP triggered an initial increase in firing rate by 416 ± 61% that remained at 415 ± 63% for 2 d in the presence of the GABAR blockers ($P < 0.001$; Fig. 1*F*), suggesting selective $GABA_BR$ blockade truly disrupts firing rate renormalization. Altogether, these results demonstrate that ongoing $GABA_BR$ activity is required for firing rate homeostasis in hippocampal networks.

**$GB_{1a}$-Containing $GABA_BRs$ Mediate Homeostatic Increase in Evoked Vesicle Release.** What are the mechanisms underlying disruption of firing rate homeostasis by $GABA_BR$ blockade? To address this question, we assessed the dependency of synaptic homeostatic responses that normally contribute to firing rate homeostasis on the $GABA_BR$ function during activity changes. As a perturbation, we applied tetrodotoxin for 48 h ($TTX_{48h}$) to silence spiking activity, a classical paradigm in homeostasis research. First, we asked whether active $GABA_BRs$ are required for inactivity-induced increase in spike-evoked vesicle exocytosis estimated by the FM1-43 method (19). To this end, the total pool of recycling vesicles was stained by maximal stimulation (600 stimuli at 10 Hz) and subsequently destained by 1 Hz stimulation (Fig. 2*A* and *SI Appendix*, Fig. S2*A*). $TTX_{48h}$ induced a 1.4-fold increase in the destaining rate constant (measured as $1/\tau_{decay}$, whereas $\tau_{decay}$ is an exponential time course) and, thus, vesicle exocytosis ($P < 0.001$; Fig. 2 *B* and *G*). However, the adaptive enhancement of release probability (*Pr*) to inactivity was abolished when neurons were treated with TTX in the presence of CGP over the course of 48 h [$(TTX + CGP)_{48h}$; $P > 0.4$; Fig. 2 *C* and *G*]. Importantly, CGP application acutely increased FM destaining rate ($P < 0.01$; *SI Appendix*, Fig. S2*B*), which remained elevated for 48 h in the presence of CGP ($CGP_{48h}$; $P < 0.01$; Fig. 2 *C* and *G*), indicating that the expected compensatory reduction in *Pr* was impaired under the $GABA_BR$ blockade. Acute application of CGP after $TTX_{48h}$ treatment during FM destaining did not alter adaptive increase in vesicle exocytosis (*SI Appendix*, Fig. S2*C*). It is noteworthy that *Pr* was not saturated under $GABA_BR$ blockade, as presynaptic homeostatic compensation by $TTX_{48h}$ was normally expressed in high-*Pr* boutons under elevated extracellular $Ca^{2+}$ levels (Fig. 2 *D* and *G* and *SI Appendix*, Fig. S2*D*). Moreover, $GABA_AR$ blockade by gabazine for 48 h induced an adaptive reduction in *Pr* that was prevented by CGP coapplication (*SI Appendix*, Fig. S3). Thus, the failure in the homeostatic mechanisms is not associated with modulation of basal *Pr*. Taken together, these results indicate that basal $GABA_BR$ activity is necessary to achieve a compensatory increase in spike-evoked synaptic vesicle exocytosis in hippocampal synapses.

Which isoform of the $GABA_BRs$ mediates homeostatic increase in evoked vesicle release? $GABA_BRs$ are obligatory heterodimers, requiring two homologous subunits, $GB_1$ and $GB_2$, for functional expression (20). In hippocampal synapses, the $GB_{1a}$ isoform is predominantly expressed at glutamatergic presynaptic

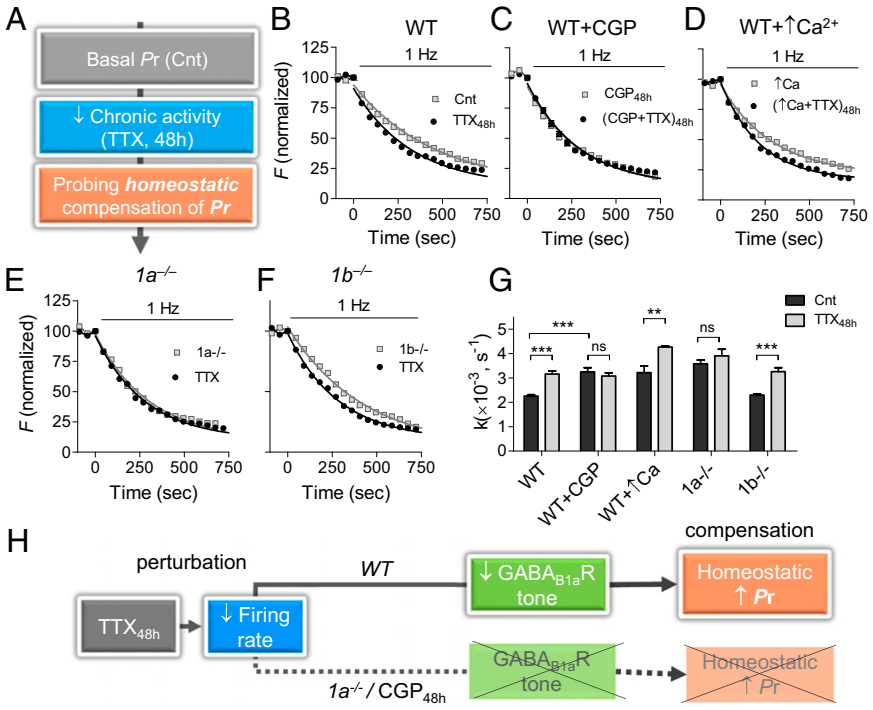


**Fig. 2.** Presynaptic homeostatic response is impaired by $GABA_BR$ blockade or $GB_{1a}$ deletion. (*A*) Experimental protocol for determining changes in synaptic vesicle exocytosis after prolonged inactivity by $TTX_{48h}$ (0.5 μM, 48 h). (*B–F*) Representative FM destaining rate curves of 50 synapses incubated with/without $TTX_{48h}$ in WT neurons (*B*), WT neurons treated by $CGP_{48h}$ (1 μM CGP for 48 h; *C*), WT neurons grown in increased (2 mM) $Ca^{2+}$ concentration (*D*), $1a^{-/-}$ neurons (*E*), and $1b^{-/-}$ neurons (*F*). (*G*) Effect of $TTX_{48h}$ on average destaining rate constants in WT neurons ($n = 687–701$), WT neurons incubated with $CGP_{48h}$ ($n = 593–748$), WT neurons in presence of high $Ca^{2+}$ ($n = 278–331$), $1a^{-/-}$ neurons ($n = 313–327$), and $1b^{-/-}$ neurons ($n = 303–313$). (*H*) Schematic illustration of $TTX_{48h}$-induced *Pr* homeostatic regulation by neuronal inactivity via $GABA_{B1a}Rs$.

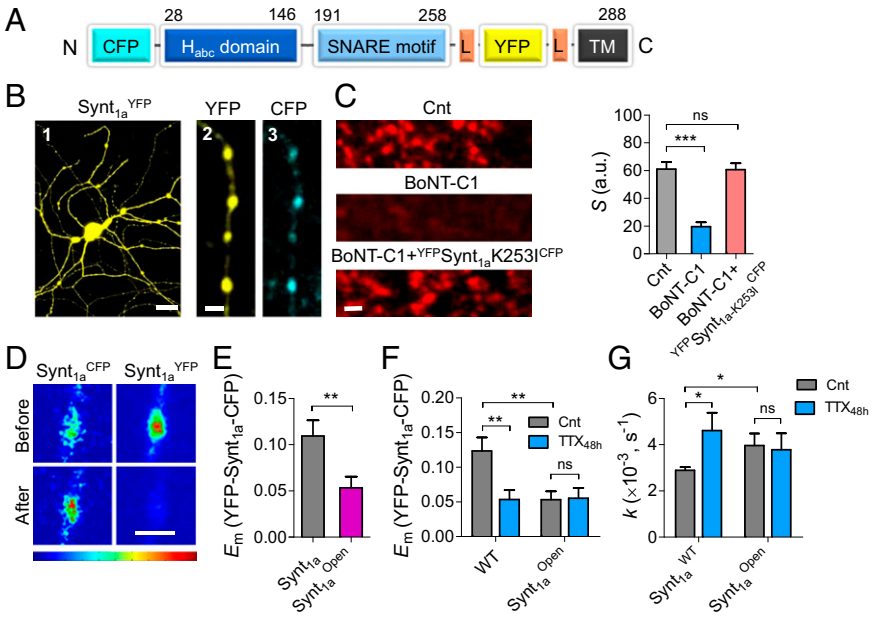


**Fig. 3.** Homeostatic mechanisms promote closed-to-open $Synt_{1a}$ conformational switch by neuronal inactivity. (*A*) Schematic illustration of $Synt_{1a}$ FRET construct (27). (*B*) Representative confocal image of a hippocampal neuron transfected with CFP-$Synt_{1a}$-YFP and zoom-in image of an axon. (*C*, *Left*) Synaptic vesicle recycling is blocked in neurons expressing BoNT-C1 light chain but is rescued by CFP-$Synt_{1a}$-K253I-YFP FRET probe. FM4-64 staining during 20-Hz stimulation (600 APs). (*Right*) Quantification of total presynaptic strength (*S*) in neurons expressing (*1*) CFP only (Cnt, $n = 8$) (*2*), BoNT-C1 ($n = 12$), and (*3*) BoNT-C1 + CFP-$Synt_{1a}$-K253I-YFP FRET probe ($n = 9$). (*D*) Pseudocolor-coded fluorescent images of CFP-$Synt_{1a}$-YFP protein expressing bouton before and after YFP photobleaching. (*E*) $Synt_{1a}^{Open}$ reduces $E_m$ ($n = 30$–$38$). (*F*) Summary of the $TTX_{48h}$ effect in neurons expressing wild-type $Synt_{1a}$ probe ($n = 23$–$34$) and $Synt_{1a}^{Open}$ ($n = 38$–$25$). (*G*) Average destaining rate constants in $Synt_{1a}^{WT}$ ($n = 284$), $Synt_{1a}^{WT}$ treated by $TTX_{48h}$ ($n = 181$), $Synt_{1a}^{Open}$ ($n = 270$), and $Synt_{1a}^{Open}$ treated by $TTX_{48h}$ ($n = 192$). [Scale bars, 20 μm (*B*, *1*) and 2 μm (*B*, *2* and *3*, and *D*)].

boutons, whereas $GB_{1b}$ is predominantly expressed at spines (21). Thus, we examined whether the presynaptic homeostatic response is disrupted in $1a^{-/-}$ boutons lacking the $GB_{1a}$ receptor subunit (21). The $1a^{-/-}$ boutons did not display a presynaptic response to activity blockade (Fig. 2 *E* and *G*). The deficits in presynaptic homeostatic plasticity were specific for the $GB_{1a}$ isoform, as $1b^{-/-}$ boutons displayed a typical adaption to prolonged synaptic inactivity (Fig. 2 *F* and *G*). Notably, acute application of CGP increased evoked synaptic vesicle release in the wild-type and $1b^{-/-}$, but not $1a^{-/-}$, boutons (*SI Appendix*, Fig. S4), confirming that the $GB_{1a}$-containing receptors mediate inhibition of *Pr* by local GABA levels. Although our previous data demonstrated a correlation between inactivity-induced reduction in the $GB_{1a}$ receptor activity and increase in *Pr* (22), our current results suggest that the basal $GB_{1a}$ receptor activity is required for homeostatic *Pr* regulation (Fig. 2*H*).

In contrast to inactivity-induced regulation of spike-evoked vesicle exocytosis, neither acute (*SI Appendix*, Fig. S5) nor chronic (*SI Appendix*, Fig. S6) application of CGP affected miniature excitatory postsynaptic current (mEPSC) frequency. Moreover, $TTX_{48h}$ alone or in the presence of $CGP_{48h}$ did not significantly change mEPSC frequency (*SI Appendix*, Fig. S6). It is worth mentioning that $TTX_{48h}$ reduced short-term synaptic facilitation during spike bursts measured by double-patch recordings (*SI Appendix*, Fig. S7), indicating an increase in *Pr* (23). Thus, the difference between spike-evoked and spontaneous vesicle release regulation observed under our experimental conditions reflects differential regulation of exocytosis during spontaneous and evoked synaptic activity (24). Although $GABA_BR$ blockade did not affect regulation of mEPSC frequency, it impaired inactivity-induced increase in mEPSC amplitude, suggesting the postsynaptic $GABA_BRs$ are involved in this regulation. Indeed, the effect of $TTX_{48h}$ was absent in $1b^{-/-}$ neurons (*SI Appendix*, Fig. S8), suggesting the $GB_{1b}$-containg postsynaptic $GABA_BRs$ play an important role in synaptic scaling.

**Inactivity Promotes Syntaxin-1 Conformational Switch.** What are the molecular mechanisms underlying the homeostatic increase in *Pr* by presynaptic $GABA_BRs$? SNARE-complex assembly is initiated by a syntaxin-1 ($Synt_1$) switch from its closed conformation (in which the N-terminal $H_{abc}$ domain of $Synt_1$ folds back onto its SNARE domain) into an open conformation (in which the SNARE domain becomes unmasked for SNARE-complex formation) (25). Rendering $Synt_1$ constitutively open induces an increase in *Pr* by enhancing SNARE-complex assembly per vesicle (26). However, activity-dependent mechanisms regulating $Synt_1$ conformational switch are not fully understood.

To assess whether chronic inactivity promotes $Synt_1$ opening, we used a recently developed intramolecular $Synt_{1a}$ FRET probe (CFP-$Synt_{1a}$-YFP) that reports the closed-to-open transition as a decrease in FRET efficiency (27). The $Synt_{1a}$ sensor contains CFP fluorophore inserted at the N terminus and YFP inserted after the SNARE motif (Fig. 3*A*) and is well expressed in processes of hippocampal neurons (Fig. 3*B*). The engineered $Synt_{1a}$ FRET reporter has been shown to assemble into endogenous SNARE complexes and was able to reconstitute dense-core vesicle exocytosis in PC12 cells (27). Furthermore, we show that neurons transfected with the light chain of BoNT-C1 are not capable of synaptic vesicle recycling, even during strong stimulation (600 pulses at 20 Hz; Fig. 3*C*). However, coexpression of BoNT-C1, together with BoNT-C1-insensitive CFP-$Synt_{1a}$K253I-YFP mutant reporter, restores synaptic vesicle recycling to the level observed in wild-type neurons (Fig. 3*C*). These results strongly suggest the CFP-$Synt_{1a}$-YFP FRET reporter is functional, supporting synaptic vesicle exocytosis in hippocampal neurons.

To monitor $Synt_{1a}$ conformational changes, we measured the steady-state FRET efficiency ($E_m$), using the acceptor photobleaching method at presynaptic boutons expressing CFP-$Synt_{1a}$-YFP

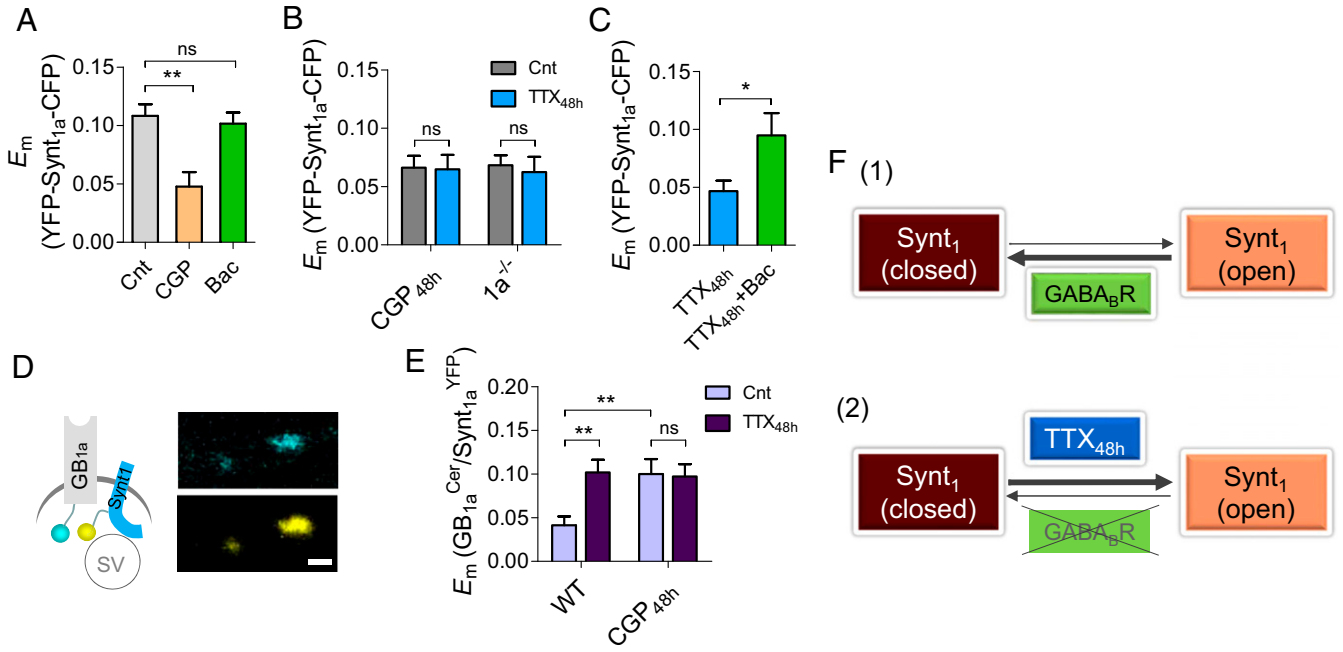


**Fig. 4.** Neuronal inactivity promotes $Synt_1$ opening by removal of $GABA_BR$-mediated block. (*A*) Acute application of CGP reduced CFP-$Synt_{1a}$-YFP $E_m$ ($n = 38$), whereas 10 μM baclofen did not affect it ($n = 88$) in WT neurons. (*B*) Summary of the $TTX_{48h}$ effect on CFP-$Synt_{1a}$-YFP $E_m$ in the presence of $CGP_{48h}$ in WT ($n = 42$–45) and in $1a^{-/-}$ ($n = 40$–80) neurons. (*C*) Baclofen (10 μM) rescued $TTX_{48h}$-induced FRET reduction ($n = 25$–40). (*D*) Representative confocal images of boutons cotransfected with $GB_{1a}^{Cer}$ and $Synt_{1a}^{YFP}$. (Scale bar, 1 μm.) (*E*) Effect of $TTX_{48h}$ on $GB_{1a}^{Cer}/Synt_{1a}^{YFP}$ $E_m$ ($n = 48$–57). $CGP_{48h}$ increases $GB_{1a}^{Cer}/Synt_{1a}^{YFP}$ $E_m$ and abolishes $TTX_{48h}$-induced $E_m$ changes ($n = 41$–69). (*F*) Schematic illustration of $Synt_1$ conformational switch regulation by neuronal inactivity via $GABA_BRs$.

(Fig. 3*B*, *2* and *3*). High-magnification confocal images show an increase in CFP fluorescence after YFP photobleaching (Fig. 3*D*), indicating dequenching of the donor and the presence of FRET. On average, CFP-$Synt_{1a}$-YFP FRET efficiency across hippocampal boutons was 0.12 ± 0.02 (Fig. 3*E*). To validate that the probe reports closed-to-open transition as a decrease in FRET efficiency, we used the $Synt_{1a}^{Open}$ FRET probe with L165E/L166E mutations, rendering $Synt_1$ in a constitutively open conformation (25). Indeed, $Synt_{1a}^{Open}$ displayed 56% lower FRET efficiency in comparison with the wild-type $Synt_{1a}$ probe (0.053 ± 0.01; $P <$ 0.01; Fig. 3*E*).

Next, we asked whether $Synt_{1a}$ conformation is homeostatically regulated by chronic neuronal inactivity to promote *Pr* augmentation. Indeed, $TTX_{48h}$ induced a reduction in $Synt_{1a}$ FRET to 0.05 ± 0.01 ($P < 0.01$; Fig. 3*F*). Notably, the reduction magnitude by $TTX_{48h}$ was similar to that exhibited by $Synt_{1a}^{Open}$ and was occluded by $Synt_{1a}^{Open}$. At the functional level, $Synt_{1a}^{Open}$ increased the rate of vesicle exocytosis ($P < 0.05$; Fig. 3*G*), supporting results of earlier studies (26, 28). Most important, $Synt_{1a}^{Open}$ occluded the effect of $TTX_{48h}$ on *Pr* ($P > 0.7$; Fig. 3*G*), suggesting a functional importance of $Synt_{1a}$ opening in compensatory *Pr* augmentation.

**Removal of $GABA_BR$ Block Mediates Inactivity-Induced Syntaxin-1 Opening.** To examine whether $GABA_BR$ tone is required for inactivity-induced $Synt_{1a}$ opening, we first asked whether $Synt_{1a}$ conformation is regulated by basal $GABA_BR$ activity. Acute application of $GABA_BR$ antagonist CGP reduced mean FRET level to 0.048 ± 0.01 ($P < 0.01$; Fig. 4*A*). Application of $GABA_BR$ agonist baclofen (10 μM) did not affect FRET ($P >$ 0.05; Fig. 4*A*), indicating that basal GABA levels are sufficient to stabilize a closed $Synt_{1a}$ conformation. Next, we asked whether $GABA_BR$ blockade interferes with $TTX_{48h}$-induced $Synt_{1a}$ opening. $CGP_{48h}$ caused a reduction in $Synt_{1a}$ FRET ($P < 0.01$; Fig. 4*B*) and occluded the effect of $TTX_{48h}$ on $Syn_{1a}$ conformational change (Fig. 4*B*). The effect of $CGP_{48h}$ was mimicked by deletion of the $GB_{1a}$ receptor subunit: $Synt_{1a}$ FRET was twofold lower in $1a^{-/-}$ boutons and insensitive to chronic reduction in spiking activity by $TTX_{48h}$ (Fig. 4*B*). Importantly, acute application of baclofen restored $Synt_{1a}$ FRET in $TTX_{48h}$-treated neurons (Fig. 4*C*), suggesting prolonged silencing may promote $Synt_{1a}$ opening by reducing the extracellular GABA levels (22).

Having established the necessity for $GB_{1a}$-containing $GABA_BRs$ in the homeostatic conformational change of $Synt_{1a}$, we explored a possibility of $Synt_{1a}$ and $GB_{1a}$ interactions. To quantify activity-dependent changes in $GB_{1a}$–$Synt_{1a}$ interactions at individual presynaptic sites, we used the FRET approach. To preserve the functionality of the $Synt_{1a}$ FRET reporter, we replaced CFP by its nonfluorescent mutant CFP-W66A, and a Cerulean (Cer)-tagged $GB_{1a}$ subunit at the C terminus ($GB_{1a}^{Cer}$) was used as a donor (Fig. 4*D*). Basal $GB_{1a}^{Cer}/Synt_{1a}^{YFP}$ FRET efficiency was 0.04 ± 0.01 and underwent a 2.4-fold increase by $TTX_{48h}$ ($P < 0.01$; Fig. 4*E*). Notably, blockade of $GABA_BRs$ produced a similar effect ($P < 0.01$; Fig. 4*E*), indicating that $GB_{1a}/Synt_{1a}$ interactions are regulated by basal GABA. Moreover, $CGP_{48h}$ occluded $TTX_{48h}$-induced $GB_{1a}^{Cer}/Synt_{1a}^{YFP}$ FRET changes ($P = 0.9$; Fig. 4*E*). To determine the existence of endogenous protein complexes containing $Synt_1$ and $GABA_BRs$, we performed coimmunoprecipitation experiments with solubilized mouse brain membranes. Anti-$Synt_1$ antibodies coprecipitated a significant amount of $GB_1$ proteins together with $Synt_1$ from WT, but not from full $GB_1$-KO mice (*SI Appendix*, Fig. S9). Taken together, these results indicate that $Synt_{1a}$ conformational change constitutes a critical step in presynaptic homeostatic response, that basal $GABA_BR$ activity maintains $Synt_{1a}$ in a closed conformation (Fig. 4*F*, *1*), and that prolonged inactivity removes a $GABA_BR$-imposed clamping of a closed $Synt_{1a}$ conformation, allowing $Synt_{1a}$ shift toward its open conformation (Fig. 4*F*, *2*).

**$GB_{1a}$ Is Required for Homeostatic Increase in Presynaptic Calcium Flux.** Next, we examined whether the $GB_{1a}$ receptor subunit controls homeostatic regulation of presynaptic $Ca^{2+}$ transients (29),

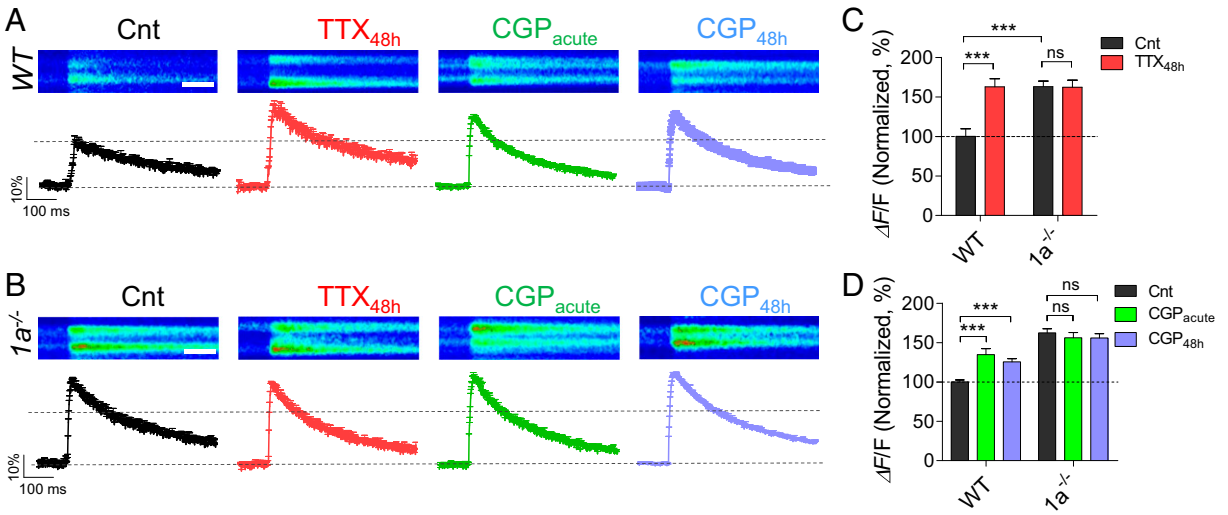


**Fig. 5.** Homeostatic increase in presynaptic calcium flux is impaired by $GB_{1a}$ deletion. (*A* and *B*) $TTX_{48h}$ increased spike-dependent presynaptic $Ca^{2+}$ entry in boutons of WT, but not in $1a^{-/-}$ neurons. (*Top*) Representative images of $Ca^{2+}$ transients (average of seven traces) evoked by 0.2-Hz stimulation during a 500-Hz line scan in boutons under control, or $TTX_{48h}$, $CGP_{acute}$, and $CGP_{48h}$ conditions in WT (*A*) and $1a^{-/-}$ (*B*) neurons. (Scale bar, 100 ms.) (*Bottom*) Averaged $Ca^{2+}$ transients, quantified as $\Delta F/F$, in control ($n = 20$), $TTX_{48h}$ ($n = 15$), $CGP_{acute}$ ($n = 29$), and $CGP_{48h}$ ($n = 37$) conditions in WT (*A*) and $1a^{-/-}$ (*B*, $n = 20$, 21, 23, and 66 for Cnt, $TTX_{48h}$, $CGP_{acute}$, and $CGP_{48h}$, respectively) neurons. (*C*) Summary of $TTX_{48h}$ effect (percentage of control) on $Ca^{2+}$ transients in boutons of WT versus $1a^{-/-}$ neurons (the same data as in *A* and *B*). Note that $Ca^{2+}$ transients were higher in $1a^{-/-}$ boutons than in WT ones. (*D*) Summary of $CGP_{acute}$ and $CGP_{48h}$ effects (percentage of control) on $Ca^{2+}$ transients in WT versus $1a^{-/-}$ boutons (the same data as in *A* and *B*).

in addition to regulating $Synt_1$ conformational switch, to adapt *Pr* to chronic activity perturbations. Thus, we measured presynaptic $Ca^{2+}$ transients evoked by 0.1-Hz stimulation, using high-affinity fluorescent calcium indicator Oregon Green 488 BAPTA-1 AM (Fig. 5*A*) at functional boutons identified by the FM4-64 marker. Although the size of action-potential dependent fluorescence transients ($\Delta F/F$) varied between different boutons, presynaptic $Ca^{2+}$ flux was significantly larger in $TTX_{48h}$-treated WT neurons ($P < 0.0001$; Fig. 5 *A* and *C*). Importantly, presynaptic $Ca^{2+}$ flux was higher in boutons of $1a^{-/-}$ neurons ($P < 0.0001$; Fig. 5 *B* and *C*), occluding the effect of $TTX_{48h}$ on further potentiation of calcium transients. It is noteworthy that $Ca^{2+}$ transients were not saturated by single action potential in $1a^{-/-}$ boutons (*SI Appendix*, Fig. S10). Furthermore, acute application of CGP increased presynaptic $Ca^{2+}$ flux that remained stable over the course of 2 d in the presence of CGP in WT ($P < 0.001$; Fig. 5 *A* and *D*), but not in $1a^{-/-}$ ($P > 0.4$; Fig. 5 *B* and *D*), neurons. This lack of compensation at the level of $Ca^{2+}$ flux was specific for the $GABA_BR$ deficit, as $GABA_AR$ blockade by gabazine has been previously shown to trigger an adaptive reduction in presynaptic $Ca^{2+}$ transients (29). These results indicate that $GB_{1a}$-containing $GABA_BRs$ normally inhibit presynaptic $Ca^{2+}$ flux evoked by single action potential and that removal of the $GABA_BR$-mediated block is essential for homeostatic potentiation of $Ca^{2+}$ flux by chronic inactivity.

**$GB_{1a}$PCT Mediates Presynaptic Homeostatic Response.** Next, we searched for the molecular domain in the $GB_{1a}$ protein that mediates the presynaptic homeostatic response. In our previous work, we identified the proximal C-terminal domain of the $GB_{1a}$ protein (R857-S877; $GB_{1a}$PCT; Fig. 6*A*) as essential for the compartmentalization of the presynaptic signaling complex of $GABA_BRs$, Gβγ G protein subunits, and $Ca_V2.2$ channels in hippocampal boutons (30). Interestingly, deletion of $GB_{1a}$PCT domain specifically impaired $Ca_V2.2$/Gβγ interaction and function, leaving $G\alpha_{i/o}$-dependent signaling unaltered.

First, we assessed the functional role of the $GB_{1a}$PCT domain in the homeostatic increase of *Pr* by comparing the effect of $TTX_{48h}$ on FM4-64 destaining rates in $1a^{-/-}$ neurons transfected with $GB_{1a}$WT-CFP versus $GB_{1a}\Delta$PCT-CFP proteins. Expression of the $GB_{1a}$WT-CFP protein rescued inactivity-induced potentiation of vesicle exocytosis in $1a^{-/-}$ neurons ($P < 0.01$; Fig. 6 *B* and *D* in comparison with Fig. 2*G*). In contrast, $TTX_{48h}$-induced presynaptic enhancement remained impaired in boutons expressing $GB_{1a}\Delta$PCT-CFP ($P > 0.8$; Fig. 6 *C* and *D*). Moreover, deletion of the $GB_{1a}$PCT domain abolished inactivity-induced increase in presynaptic calcium transients ($P > 0.8$; Fig. 6 *E*–*G*). Thus, the $GB_{1a}$PCT domain is necessary for presynaptic adaptations to prolonged inactivity in hippocampal networks.

Finally, we examined whether inactivity induces conformational $GABA_BR/Ca_V2.2$ changes, and if so, whether the $GB_{1a}$PCT domain is involved in this homeostatic regulation. We monitored FRET efficiency between the YFP-tagged $GB_{1a}$ receptor subunit at the C terminus and the CFP-tagged α1 subunit of the $Ca_V2.2$ channel at the N terminus ($GB_{1a}^{YFP}/Ca_V2.2^{CFP}$). $TTX_{48h}$ induced an increase in $GB_{1a}^{YFP}/Ca_V2.2^{CFP}$ FRET ($P < 0.05$; Fig. 6*H*), indicating that chronic neuronal silencing alters $GB_{1a}/Ca_V2.2$ interactions. Importantly, deletion of the $GB_{1a}$PCT domain disrupted $TTX_{48h}$-induced homeostatic $GB_{1a}^{YFP}/Ca_V2.2^{CFP}$ changes ($P = 0.49$; Fig. 6*H*). Moreover, $GB_{1a}$PCT deletion occluded $TTX_{48h}$-induced homeostatic $GB_{1a}^{Cer}/GB_2^{Cit}$ and $GB_{1a}^{YFP}/Synt_{1a}^{CFP}$ changes (*SI Appendix*, Fig. S11). A physical interaction between endogenous $GABA_BRs$ and $Ca_V2.2$ was revealed by coimmunoprecipitation experiments (*SI Appendix*, Fig. S9), confirming previous proteomic data (31). These results suggest that homeostatic mechanisms modulate $GB_{1a}/Ca_V2.2$ and $GB_{1a}/Synt_{1a}$ interactions in the $GABA_BR$ presynaptic signaling complex via the $GB_{1a}$PCT domain.

## Discussion

The ability of neuronal circuits to stabilize their firing properties in the face of environmental or genetic changes is critical for normal neuronal functioning. Despite extensive research on a wide repertoire of possible homeostatic mechanisms, the key regulators of firing rate homeostasis in mammalian central neural circuits remain obscure. In this work, we identified the $GABA_BR$ as a key homeostatic signaling molecule stabilizing mean firing rate in hippocampal networks. $GABA_BRs$ enable inactivity-induced homeostatic increase in synaptic strength by three principle mechanisms:

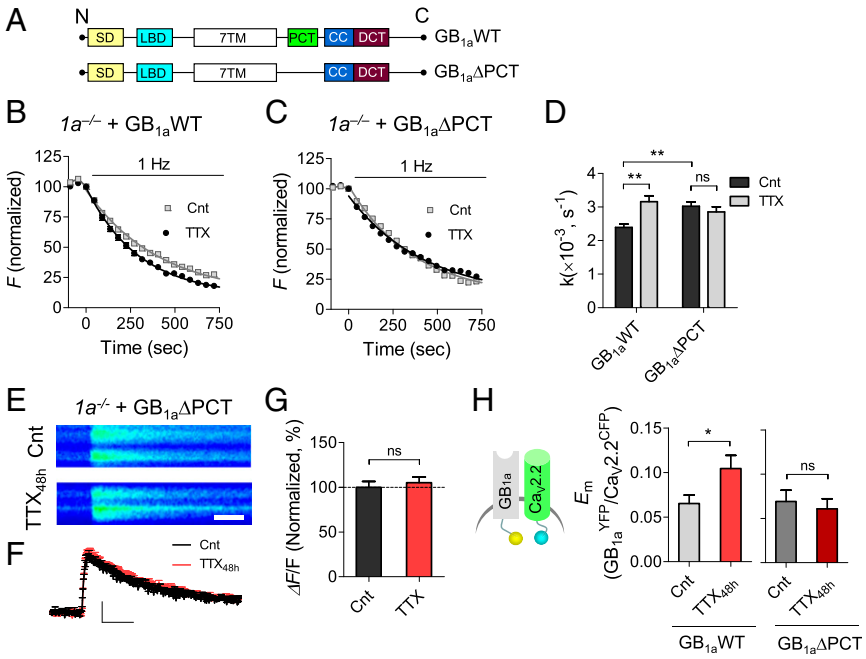


**Fig. 6.** The $GB_{1a}$PCT domain is required for presynaptic homeostatic response. (*A*) Schematics show $GB_{1a}$WT and $GB_{1a}$ΔPCT constructs. 7TM, seven-transmembrane domain; CC, coiled-coiled domain; DCT, distal C-terminal domain; LBD, ligand-binding domain; PCT, proximal C-terminal domain; SD, two sushi domains. (*B* and *C*) Representative FM destaining rate curves of 50 synapses pretreated with/without $TTX_{48h}$ in $1a^{-/-}$ neurons transfected with $GB_{1a}$WT (*B*) or $GB_{1a}$ΔPCT (*C*). (*D*) Expression of $GB_{1a}$WT ($n$ = 609–642), but not of $GB_{1a}$ΔPCT ($n$ = 598–721), restores presynaptic homeostatic adaptation in $1a^{-/-}$ neurons. (*E* and *F*) $TTX_{48h}$ did not alter spike-dependent presynaptic $Ca^{2+}$ entry in boutons expressing $GB_{1a}$ΔPCT in $1a^{-/-}$ neurons. Representative images of $Ca^{2+}$ transients (average of seven traces) evoked by 0.2-Hz stimulation in boutons of control and $TTX_{48h}$-treated $GB_{1a}$ΔPCT-expressing boutons (*E*). Averaged $Ca^{2+}$ transients in control ($n$ = 44) and $TTX_{48h}$ ($n$ = 37) conditions (*F*). (*G*) Summary of $TTX_{48h}$ effect on $Ca^{2+}$ transients in boutons expressing $GB_{1a}$ΔPCT protein (the same data as in *F*). (*H*) Effect of $TTX_{48h}$ on $GB_{1a}{}^{YFP}/Ca_V2.2^{CFP}$ $E_m$ ($n$ = 40–88). Deletion of PCT domain abolishes $TTX_{48h}$-induced change in $GB_{1a}{}^{YFP}/Ca_V2.2^{CFP}$ $E_m$ ($n$ = 44–55).

promoting synatxin-1 conformational switch to enhance SNARE-complex assembly, augmenting presynaptic $Ca^{2+}$ flux to promote spike-evoked vesicle exocytosis, and increasing the quantal excitatory amplitude. Thus, $GABA_BRs$, in addition to modulation of short-term (32, 33) and long-term, Hebbian (21) synaptic plasticity, are essential for maintaining firing stability of neural circuits.

**$GABA_BRs$ and Synaptic Homeostatic Plasticity.** Homeostatic regulation of synaptic strength represents a basic mechanism of neuronal adaptation to constant changes in ongoing activity levels. Strong evidence exists on homeostatic augmentation of *P*r and readily releasable pool size in response to prolong inactivity in hippocampal neurons (19, 22, 34–42). These homeostatic adaptations are associated with modulation of presynaptic $Ca^{2+}$ flux (29) and remodeling of a large number of proteins in presynaptic cytomatrix (7). Recent studies have identified the mechanisms underlying presynaptic homeostatic signaling in *Drosophila* neuromuscular junction, implicating epithelial sodium leak channels (43) and endostatin (44) as homeostatic regulators of the presynaptic $Ca_V2$ channels (for review, see ref. 5). However, the critical molecules controlling presynaptic homeostasis in mammalian central synapses are not fully understood.

In this work, we show that chronic neuronal silencing induces an adaptive increase in evoked basal vesicle release through $GABA_BRs$ by removing tonic inhibition of $Synt_1$ conformational switch and of presynaptic $Ca^{2+}$ flux. These results are important for several reasons. First, they reveal a crucial role for $GABA_BRs$ in presynaptic homeostasis. Taking into account a wide variety of G protein-coupled receptors that mediate presynaptic inhibition, the requirement for the $GABA_BR$ tone in presynaptic homeostatic response is particularly striking. Second, they demonstrate, for the first time, the role of the extracellular GABA in determining $Synt_1$ conformation via the presynaptic $GB_{1a}$-containing $GABA_BRs$. Either genetic $GB_{1a}$ deletion or pharmacological $GABA_BR$ blockade stabilizes an open $Synt_1$ conformation in analogy to mutations rendering $Synt_1$ constitutively open, occluding adaptive response to neuronal silencing. Notably, addition of $GABA_BR$ agonist after prolonged inactivity stabilizes a closed $Synt_1$ conformation, suggesting reduction in local GABA levels induces an adaptive $Synt_{1a}$ response. Third, in addition to the well-known role of $GABA_BRs$ in the presynaptic $Ca^{2+}$ flux inhibition, at a rapid timescale of minutes (22, 45), our work revealed the necessity for basal $GABA_BR$ activity in presynaptic adaptations of $Ca^{2+}$ transients to chronic activity perturbations at extended timescales of days. Deletion of the $GB_{1a}$PCT domain blocks presynaptic homeostatic plasticity by disrupting GABA-mediated conformational changes within the presynaptic $GB_{1a}$/$Ca_V2.2$/$Synt_1$ signaling complex. Thus, endogenous molecular "brakes" imposed by $GABA_BRs$ on $Ca_V2.2$ channels and SNARE complex assembly are essential for presynaptic homeostasis in hippocampal neurons.

It is important to note that in the present study, chronic inactivity by TTX induced a compensatory increase in mEPSC amplitude via the postsynaptic $GB_{1b}$-containing receptors without affecting mEPSC frequency. Given a pronounced effect of $TTX_{48h}$ on spike-evoked synaptic vesicle exocytosis, these results suggest complete blockade of spikes does not trigger compensatory changes in spontaneous vesicle release. In previous studies, mEPSC frequency was found to be immune to chronic TTX treatment in some cases (18, 41), while being up-regulated by AMPA receptor blockade (36, 41), either by suppression of neuronal excitability (38) or by increase in the $GABA_BR$-mediated inhibition (9). Thus, the induction of presynaptic homeostatic changes may require minimal spiking activity (41).

**$GABA_BR$-Mediated Neuronal Homeostasis and Brain Disorders.** It is tempting to speculate that many distinct neurologic and psychiatric disorders with different etiologies share common dysfunctions in pathways related to homeostatic plasticity. However, the molecular mechanisms by which defective homeostatic signaling may lead to common disease pathophysiology remain to be determined. Only a few molecular links, such as the schizophrenia-associated gene dysbindin, have been established between homeostatic system impairments and brain dysfunctions (46). Our study demonstrates that ongoing $GABA_BR$ activity is essential for population firing rate homeostasis in hippocampal networks. This may explain why aberrant neuronal activity remains uncompensated in mice lacking functional $GABA_BRs$ as a result of deletion of either the $GB_1$ (13) or $GB_2$ (15) receptor subunit. Interestingly, $1a^{-/-}$, but not $1b^{-/-}$, mice exhibit spontaneous epileptiform activity (16), suggesting the presynaptic $GB_{1a}$-containing receptors may play a more prominent role in firing rate homeostasis. Strikingly, our results show that homeostatic plasticity is impaired in synaptic networks displaying enhanced ongoing synaptic $Ca^{2+}$ flux because of removal of the $GABA_BR$-mediated block. Thus, $Ca_V2$ channel gain of function may be as detrimental for neuronal homeostasis as $Ca_V2$ loss of function (47, 48), indicating that an optimal level of ongoing synaptic $Ca^{2+}$ flux may be essential for homeostatic regulation. It remains to be seen whether the loss of functional $GABA_BRs$, associated with epilepsy and a wide range of psychiatric disorders (49), contributes to pathophysiology shared by these disorders through erasing critical pathways in homeostatic control systems.

## Materials and Methods

**Hippocampal Cell Culture.** Primary cultures of CA3-CA1 hippocampal neurons were prepared from WT, $1a^{-/-}$, and $1b^{-/-}$ (BALB/c background) mice (21) on postnatal days 0–2, as described (50). The experiments were performed in mature (14–28 d in vitro) cultures. All animal experiments were approved by the Tel Aviv University Committee on Animal Care.

**MEA Preparation and Recordings.** Cultures were plated on MEA plates containing 59 TiN recording and one internal reference electrodes [Multi Channel Systems (MCS)]. Electrodes are 30 μm in diameter and spaced 500 μm apart. Data were acquired using a MEA1060-Inv-BC-Standard amplifier (MCS) with frequency limits of 5,000 Hz and a sampling rate of 10 kHz per electrode mounted on an Olympus IX71 inverted microscope. Recordings were carried out under constant 37 °C and 5% $CO_2$ conditions, identical to incubator conditions. Spike sorting and analysis are described in ref. 9 and in *SI Appendix, Spike Sorting and Data Analysis*.

**Molecular Biology.** $GB_{1a}$WT-, $GB_{1a}$ΔPCT-, $GB_2$-, and $Ca_V2.2$-tagged proteins used throughout the study were constructed as described before (30). $Synt_{1a}$ (CSYS-5RK), $Synt_{1a}^{Open}$, and $Synt_{1a}$K253I are as described in ref. 27. W66A point mutation was introduced to silence YFP in the YFP-$Synt_{1a}$-CFP construct (Fig. 4 *D* and *E* and *SI Appendix*, Fig. S11). BoNT/C1α-51-IRES-EGFP was designed and then generated by ProGen Israel, Protein and Gene Engineering Company. Transient cDNA transfections have been performed using Lipofectamine-2000 reagents, and neurons were typically imaged 18–48 h after transfection.

**Estimation of Synaptic Vesicle Release Using FM Dyes.** Activity-dependent FM1-43 or FM4-64 styryl dyes have been used to estimate synaptic vesicle exocytosis and presynaptic plasticity, as described (22). The experiments were conducted at room temperature in extracellular Tyrode solution containing (in mM): NaCl, 145; KCl, 3; glucose, 15; Hepes, 10; $MgCl_2$, 1.2; $CaCl_2$, 1.2, with pH adjusted to 7.4 with NaOH. The extracellular medium contained nonselective antagonist of ionotropic glutamate receptors (kynurenic acid, 0.5 mM) to block recurrent neuronal activity. Synaptic vesicles were loaded with 15 μM FM4-64 in all of the experiments with GFP/CFP/YFP transfection, whereas 10 μM FM1-43 was used in all of the nontransfected neurons.

**Detecting Presynaptic Calcium Transients.** Fluorescent calcium indicator Oregon Green 488 BAPTA-1 AM was dissolved in DMSO to yield a concentration of 1 mM. For cell loading, cultures were incubated at 37 °C for 30 min with 3 μM of this solution diluted in a standard extracellular solution. Imaging was performed using FV1000 Olympus confocal microscopes, under 488 nm (excitation) and 510–570 nm (emission), using 500-Hz line scanning.

**FRET Imaging and Analysis.** Intensity-based FRET imaging was carried as described before (22, 30). Donor dequenching resulting from the desensitized acceptor was measured from Cer/CFP emission (460–500 nm) before and after the acceptor (YFP) photobleaching. Mean FRET efficiency, $E_m$, was then calculated using the equation $E_m = 1 - I_{DA}/I_D$, where $I_{DA}$ is the peak of donor emission in the presence of the acceptor and $I_D$ is the peak after acceptor photobleaching.

**Statistical Analysis.** Error bars shown in the figures represent SEM. Where applicable, the number of experiments (cultures) or the number of boutons is defined by *n*. All the experiments were repeated at least in three different batches of cultures. One-way ANOVA analysis with post hoc Bonferroni's was used to compare several conditions. Student's unpaired, two-tailed *t* test has been used in the experiments in which two different populations of synapses were compared. Student's paired, two-tailed *t* test has been used in the experiments where before and after treatments were compared at the same population of synapses. $*P < 0.05$; $**P < 0.01$; $***P < 0.001$; ns, nonsignificant.

**ACKNOWLEDGMENTS.** This work was supported by European Research Council Starting Grant 281403 (to I. Slutsky), the Israel Science Foundation (398/13 to I.S.; 234/14 to I.L.), the Binational Science Foundation (2013244 to I. Slutsky; 2009049 to I.L.), Swiss National Science Foundation (31003A_152970 to B.B.), and the Legacy Heritage Biomedical Program of the Israel Science Foundation (1195/14 to I. Slutsky). I. Slutsky is grateful to the Sheila and Denis Cohen Charitable Trust and Rosetrees Trust of the United Kingdom for their support. I.V. is grateful to the TEVA National Network of Excellence in Neuroscience for the award of a postdoctoral fellowship.

1. Turrigiano GG, Nelson SB (2000) Hebb and homeostasis in neuronal plasticity. *Curr Opin Neurobiol* 10(3):358–364.
2. Turrigiano GG, Nelson SB (2004) Homeostatic plasticity in the developing nervous system. *Nat Rev Neurosci* 5(2):97–107.
3. Davis GW (2006) Homeostatic control of neural activity: from phenomenology to molecular design. *Annu Rev Neurosci* 29:307–323.
4. Marder E, Goaillard JM (2006) Variability, compensation and homeostasis in neuron and network function. *Nat Rev Neurosci* 7(7):563–574.
5. Davis GW, Müller M (2015) Homeostatic control of presynaptic neurotransmitter release. *Annu Rev Physiol* 77:251–270.
6. Turrigiano G (2011) Too many cooks? Intrinsic and synaptic homeostatic mechanisms in cortical circuit refinement. *Annu Rev Neurosci* 34:89–103.
7. Lazarevic V, Schöne C, Heine M, Gundelfinger ED, Fejtova A (2011) Extensive remodeling of the presynaptic cytomatrix upon homeostatic adaptation to network activity silencing. *J Neurosci* 31(28):10189–10200.
8. Ehlers MD (2003) Activity level controls postsynaptic composition and signaling via the ubiquitin-proteasome system. *Nat Neurosci* 6(3):231–242.
9. Slomowitz E, et al. (2015) Interplay between population firing stability and single neuron dynamics in hippocampal networks. *eLife* 4:e04378.
10. Hengen KB, Lambo ME, Van Hooser SD, Katz DB, Turrigiano GG (2013) Firing rate homeostasis in visual cortex of freely behaving rodents. *Neuron* 80(2):335–342.
11. O'Leary T, Williams AH, Franci A, Marder E (2014) Cell types, network homeostasis, and pathological compensation from a biologically plausible ion channel expression model. *Neuron* 82(4):809–821.
12. Ramocki MB, Zoghbi HY (2008) Failure of neuronal homeostasis results in common neuropsychiatric phenotypes. *Nature* 455(7215):912–918.
13. Schuler V, et al. (2001) Epilepsy, hyperalgesia, impaired memory, and loss of pre- and postsynaptic GABA(B) responses in mice lacking GABA(B(1)). *Neuron* 31(1):47–58.
14. Prosser HM, et al. (2001) Epileptogenesis and enhanced prepulse inhibition in GABA (B1)-deficient mice. *Mol Cell Neurosci* 17(6):1059–1070.
15. Gassmann M, et al. (2004) Redistribution of GABAB(1) protein and atypical GABAB responses in GABAB(2)-deficient mice. *J Neurosci* 24(27):6086–6097.
16. Vienne J, Bettler B, Franken P, Tafti M (2010) Differential effects of GABAB receptor subtypes, gamma-hydroxybutyric Acid, and Baclofen on EEG activity and sleep regulation. *J Neurosci* 30(42):14194–14204.
17. Badran S, Schmutz M, Olpe HR (1997) Comparative in vivo and in vitro studies with the potent GABAB receptor antagonist, CGP 56999A. *Eur J Pharmacol* 333(2-3): 135–142.
18. Turrigiano GG, Leslie KR, Desai NS, Rutherford LC, Nelson SB (1998) Activity-dependent scaling of quantal amplitude in neocortical neurons. *Nature* 391(6670): 892–896.
19. Murthy VN, Schikorski T, Stevens CF, Zhu Y (2001) Inactivity produces increases in neurotransmitter release and synapse size. *Neuron* 32(4):673–682.
20. Bettler B, Kaupmann K, Mosbacher J, Gassmann M (2004) Molecular structure and physiological functions of GABA(B) receptors. *Physiol Rev* 84(3):835–867.
21. Vigot R, et al. (2006) Differential compartmentalization and distinct functions of GABAB receptor variants. *Neuron* 50(4):589–601.

22. Laviv T, et al. (2010) Basal GABA regulates GABA(B)R conformation and release probability at single hippocampal synapses. *Neuron* 67(2):253–267.
23. Dobrunz LE, Stevens CF (1997) Heterogeneity of release probability, facilitation, and depletion at central synapses. *Neuron* 18(6):995–1008.
24. Raingo J, et al. (2012) VAMP4 directs synaptic vesicles to a pool that selectively maintains asynchronous neurotransmission. *Nat Neurosci* 15(5):738–745.
25. Dulubova I, et al. (1999) A conformational switch in syntaxin during exocytosis: role of munc18. *EMBO J* 18(16):4372–4382.
26. Acuna C, et al. (2014) Microsecond dissection of neurotransmitter release: SNARE-complex assembly dictates speed and $Ca^{2+}$ sensitivity. *Neuron* 82(5):1088–1100.
27. Greitzer-Antes D, et al. (2013) Tracking Ca2+-dependent and Ca2+-independent conformational transitions in syntaxin 1A during exocytosis in neuroendocrine cells. *J Cell Sci* 126(Pt 13):2914–2923.
28. Gerber SH, et al. (2008) Conformational switch of syntaxin-1 controls synaptic vesicle fusion. *Science* 321(5895):1507–1510.
29. Zhao C, Dreosti E, Lagnado L (2011) Homeostatic synaptic plasticity through changes in presynaptic calcium influx. *J Neurosci* 31(20):7492–7496.
30. Laviv T, et al. (2011) Compartmentalization of the GABAB receptor signaling complex is required for presynaptic inhibition at hippocampal synapses. *J Neurosci* 31(35):12523–12532.
31. Müller CS, et al. (2010) Quantitative proteomics of the Cav2 channel nano-environments in the mammalian brain. *Proc Natl Acad Sci USA* 107(34):14950–14957.
32. Varela JA, et al. (1997) A quantitative description of short-term plasticity at excitatory synapses in layer 2/3 of rat primary visual cortex. *J Neurosci* 17(20): 7926–7940.
33. Kreitzer AC, Regehr WG (2000) Modulation of transmission during trains at a cerebellar synapse. *J Neurosci* 20(4):1348–1357.
34. Lee KJ, et al. (2013) Mossy fiber-CA3 synapses mediate homeostatic plasticity in mature hippocampal neurons. *Neuron* 77(1):99–114.
35. Kim J, Tsien RW (2008) Synapse-specific adaptations to inactivity in hippocampal circuits achieve homeostatic gain control while dampening network reverberation. *Neuron* 58(6):925–937.
36. Thiagarajan TC, Lindskog M, Tsien RW (2005) Adaptation to synaptic inactivity in hippocampal neurons. *Neuron* 47(5):725–737.
37. Branco T, Staras K, Darcy KJ, Goda Y (2008) Local dendritic activity sets release probability at hippocampal synapses. *Neuron* 59(3):475–485.
38. Burrone J, O'Byrne M, Murthy VN (2002) Multiple forms of synaptic plasticity triggered by selective suppression of activity in individual neurons. *Nature* 420(6914):414–418.
39. Wierenga CJ, Walsh MF, Turrigiano GG (2006) Temporal regulation of the expression locus of homeostatic plasticity. *J Neurophysiol* 96(4):2127–2133.
40. Bacci A, et al. (2001) Chronic blockade of glutamate receptors enhances presynaptic release and downregulates the interaction between synaptophysin-synaptobrevin-vesicle-associated membrane protein 2. *J Neurosci* 21(17):6588–6596.
41. Jakawich SK, et al. (2010) Local presynaptic activity gates homeostatic changes in presynaptic function driven by dendritic BDNF synthesis. *Neuron* 68(6):1143–1158.
42. Mitra A, Mitra SS, Tsien RW (2012) Heterogeneous reallocation of presynaptic efficacy in recurrent excitatory circuits adapting to inactivity. *Nat Neurosci* 15(2):250–257.
43. Younger MA, Müller M, Tong A, Pym EC, Davis GW (2013) A presynaptic ENaC channel drives homeostatic plasticity. *Neuron* 79(6):1183–1196.
44. Wang T, Hauswirth AG, Tong A, Dickman DK, Davis GW (2014) Endostatin is a trans-synaptic signal for homeostatic synaptic plasticity. *Neuron* 83(3):616–629.
45. Wu LG, Saggau P (1995) GABAB receptor-mediated presynaptic inhibition in guinea-pig hippocampus is caused by reduction of presynaptic Ca2+ influx. *J Physiol* 485(Pt 3): 649–657.
46. Dickman DK, Davis GW (2009) The schizophrenia susceptibility gene dysbindin controls synaptic homeostasis. *Science* 326(5956):1127–1130.
47. Frank CA, Kennedy MJ, Goold CP, Marek KW, Davis GW (2006) Mechanisms underlying the rapid induction and sustained expression of synaptic homeostasis. *Neuron* 52(4): 663–677.
48. Müller M, Davis GW (2012) Transsynaptic control of presynaptic $Ca^{2+}$ influx achieves homeostatic potentiation of neurotransmitter release. *Curr Biol* 22(12): 1102–1108.
49. Gassmann M, Bettler B (2012) Regulation of neuronal GABA(B) receptor functions by subunit composition. *Nat Rev Neurosci* 13(6):380–394.
50. Slutsky I, Sadeghpour S, Li B, Liu G (2004) Enhancement of synaptic plasticity through chronically reduced Ca2+ flux during uncorrelated activity. *Neuron* 44(5): 835–849.